

Helium ions from the interaction of 70-MeV pions with nuclei*

A. Doron, A. Altman, D. Ashery, Y. Shamaï, and A. I. Yavin

Department of Physics and Astronomy, Tel Aviv University, Ramat Aviv, Israel

J. Julien, Y. Cassagnou, H. E. Jackson,[†] and R. Legrain

Département de Physique Nucléaire, Centre d'Etudes Nucléaires de Saclay, B.P. No. 2, 91190 Gif-sur-Yvette, France

A. Palmeri and S. Barbarino

Istituto Nazionale di Fisica Nucleare, Sezione di Catania, Catania 95129, Italy

(Received 19 July 1977)

He ions emitted in the interaction of 70-MeV pions with carbon, aluminum, nickel, silver, and gold were measured directly at $\theta = 90^\circ$. Cross sections and energy spectra are presented. Calculations of intranuclear cascades followed by evaporation reproduced the experimental data reasonably well. The results of the calculations imply that: (1) pion absorption in flight plays a major role in reactions in which α particles are emitted; and (2) one- α -removal lines, observed in deexcitation γ -ray experiments, do not imply large probability for real α emission. The π^- to π^+ ratio of cross sections was found to be about 1.4.

NUCLEAR REACTIONS C, Al, Ni, Ag, Au (π^+ , α + anything), $E_\pi = 70$ MeV; measured He energy spectra; $d\sigma/d\Omega(90^\circ)$. Natural targets; evaporation analysis.

I. INTRODUCTION

A rich variety of pion-nucleus reactions has been revealed in recent years by many inclusive experiments,¹⁻¹³ in which only one of the out-going particles is detected. The method most commonly used is the measurement of prompt deexcitation γ rays. Residual nuclei are identified in this method when they are left in excited states. No information is provided about the nature of the particles which are emitted prior to the γ deexcitation, and the reaction mechanism cannot be directly determined. In particular, much interest was aroused²⁻⁷ by the high relative yields of residual nuclei corresponding to the removal of three and four nucleons from the target nucleus, called " t "- (" ^3He "-) and " α "-removal reactions, respectively. At first, this seemed to suggest^{2, 5, 6, 8, 9} an interaction of pions with α clusters within the nucleus. Experimental data on p , d , and t emission⁸ were consistent with this explanation. Several authors attempted to explain data for elastic scattering,¹⁴ pion capture,¹⁵ and pionic atoms¹⁶ in an α model of the nucleus, which includes absorption of pions on α clusters (and on deuteron clusters). Recently, with the accumulation of more information, the high relative yields of t - and α -removal lines were explained by Zaider *et al.*,¹ as caused by nuclear characteristics rather than by preferential interactions. This seems to eliminate the need to assume an interaction of pions with α clusters to explain these high yields.

Previous experiments provided direct measurements of α particles emitted in the interaction of 70-MeV π^- on aluminum¹¹ and 235-MeV π^+ on nickel

and silver.¹² The analysis of the 235-MeV data seemed to suggest a pickup mechanism to explain the emission of high energy complex particles. A tentative analysis of the 70-MeV data indicated that the low energy He yield could be explained by simple evaporation following the pion-nucleus interaction. The two approaches are complementary rather than contradictory. It is evident that more data are needed before we can have a better understanding of the origin of the emitted α particles.

Inclusive particle data and inclusive γ -ray data are difficult to compare. For example, let us compare the reactions:

$$\pi^- + {}^{27}\text{Al} \rightarrow \alpha + \text{anything}, \quad (1)$$

$$\pi^- + {}^{27}\text{Al} \rightarrow \gamma({}^{23}\text{Na}) + \text{anything}, \quad (2)$$

$$\pi^- + {}^{27}\text{Al} \rightarrow \gamma({}^{23}\text{Ne}) + \text{anything}, \quad (3)$$

where $\gamma({}^AZ)$ means a deexcitation γ ray in the nucleus AZ . Reaction (1) may be observed in direct particle detection. Reactions (2) and (3), which include the process of the removal of an equivalent α cluster from the target nucleus, without and with π^- absorption, respectively, may be observed in the deexcitation γ -ray method. Since both methods are inclusive, there is only little overlap between the two measurements. The main common channels to both methods are

$$\pi^- + {}^{27}\text{Al} \rightarrow \pi^- + \alpha + \gamma({}^{23}\text{Na}) + {}^{23}\text{Na}, \quad (2a)$$

$$\pi^- + {}^{27}\text{Al} \rightarrow \alpha + \gamma({}^{23}\text{Ne}) + {}^{23}\text{Ne}. \quad (3a)$$

In principle, only limited conclusions can be drawn from inclusive measurements, in which not all of

the outgoing particles are observed. However, if an analysis can treat several inclusive reactions within the framework of the same model, a comparison of results is made possible. One of the main goals of such a program would then be to identify the major channels in each reaction and the relative strength of the common channels. The consistency of that picture would lend a measure of confidence in both model and analysis. Thus, each direct measurement of the emitted particles, though inclusive, complements other inclusive measurements, supplementing scattering data in shedding more light on the pion-nucleus interaction.

We undertook a study of α emission from pion-induced reactions. Targets of carbon, aluminum, nickel, silver, and gold were bombarded with 70-MeV pions. This energy was previously used in prompt γ measurements,¹ and a comparison is thus made possible. Measurements of total and scattering cross sections for both charges have only recently been carried out. Some pion induced reactions have shown puzzling differences between π^- and π^+ cross sections, like the π^-/π^+ ratio in nucleon knockout. Previous direct measurements of pion induced α emission were taken with only one pion charge. We therefore decided to use both pion charges. He ions were detected and their energy spectra were measured.

The experimental details of the measurements are presented in Sec. II. In Sec. III we present the results and analyze them within the framework of a model, which assumes intranuclear cascades followed by evaporation. In Sec. IV we discuss the implications of these results. The conclusions are summarized in Sec. V.

II. EXPERIMENTAL TECHNIQUE

A. Beam

We used the pion beam from the new pion-muon (PM2) channel of the electron linear accelerator at the Centre d'Études Nucléaires de Saclay. The beam at the target had a horizontal Gaussian profile of 36 mm full width at half maximum. The vertical profile was not Gaussian, and was 55 mm wide at half maximum and 114 mm wide at $\frac{1}{10}$ maximum. The beam profiles were monitored by a hodoscope made of eight horizontal and eight vertical plastic scintillators. Relative monitoring of beam intensity was achieved with a thin plastic scintillator, placed about 2 m beyond the target and somewhat off the beam-line axis to avoid the main part of the incident beam. The counting rate of this monitor was low so that pileup and dead time effects were negligible even at high pion intensities. The relative monitor was calibrated, at low pion intensities, by comparison to triple-

coincidence signals from three plastic scintillators: two scintillators at the exit port of the channel; and a third one, of target dimensions, in the target position. (This was necessary since the targets were usually smaller than the beam spot.) The linearity of the monitor was checked, relative to the primary beam intensity, up to the highest pion intensity.

Beam contamination was determined in two separate checks. In one, the profiles and intensity of the electrons (positrons) were measured using a Čerenkov counter in coincidence with the hodoscope. The electron contamination was found to be 17% of the total number of incident particles (12% e^+ in the positive pion beam). In the other check, the muon contamination was estimated from muonic x-rays detection to be 5% of the total number of particles impinging on the target. An aluminum absorber at the exit port of the beam stopped protons in the positive π beam. The duty cycle of the beam was 2% (20- μ sec bursts every 1 msec). The average intensity of the net pion beam was about $4 \times 10^5 \pi/\text{sec}$. The systematic uncertainty of the normalization, including monitoring and contaminations, was about 15%.

B. Experimental setup and electronics

The experimental setup is shown in Fig. 1. Targets of natural Al, Ni, Ag, and Au (10–20 mg/cm² thick) were used. Polyethylene was used for the C target. All foils ($\approx 10 \times 10$ cm²) were held in thin aluminum target holders, which provided an opening of 15×15 cm². The targets were tilted at 30° relative to the beam direction.

A three-counter telescope was used. All three

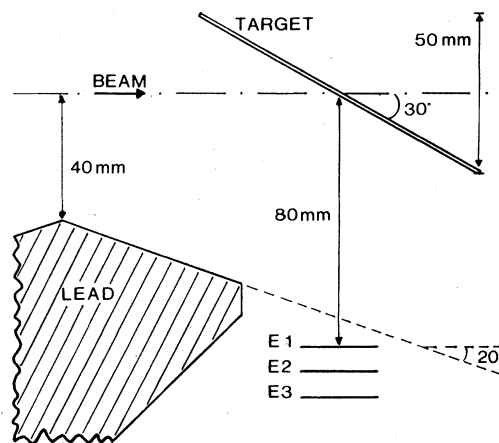


FIG. 1. Horizontal section of the experimental setup.

detectors were of silicon-surface-barrier type. The detector E_1 was 30 μm thick, with a 300-mm² sensitive area. The detector E_2 was 500 μm thick and the detector E_3 was 2000 μm thick, both of 450-mm² sensitive area. The telescope was placed at 90° to the incident beam, and its front surface was 8 cm from the center of the beam. The solid angle subtended was about 0.035 sr. The telescope was shielded from the beam by lead. The shielding was cut in a shape which minimized counts of muons and other particles from either pion decay in the beam, or muon and electron interactions with the shielding.

Counting information was stored event by event on magnetic tapes. A computer was used for data acquisition and on-line analysis. Standard CAMAC modules were used to interface the data to the computer. Logic and analogic information from the system was digitized and stored, following an event trigger from the system. Such a trigger signal was issued whenever a valid event occurred during a beam burst and no inhibition signal was present. The system was then inhibited during the conversion time in the analog-to-digital converter units and the reading cycle of the computer. A valid event was defined by the logic condition $E_1 E_2 \bar{E}_3$. He ions in the range 7–36 MeV could be detected in this configuration. Using a randomly triggered pulser signal it was found that the dead time of the system was negligible.

C. Data analysis

Particle identification was performed after the run using the standard identification function $(E_1 + E_2)^\mu - E_2^\mu$, with $\mu = 1.69$. ³He ions could not be distinguished from α particles mainly because of the geometry used. Using a Monte Carlo computer code, a particle spectrum may be simulated. This was done and effects of geometry, straggling, resolution, discrimination levels, and energy loss were taken into account. The experimental particle spectrum was found to agree very well with the simulation.

Background spectra of He ions, with an empty target holder, were taken for each pion charge, and were found to have low yields. They were smoothed out, and then subtracted from the raw spectra.

The solid angle subtended by the telescope was calculated with a Monte Carlo computer code. Beam shape and dimensions, as well as target dimensions and inclination, were taken into account when an interaction point in the target was randomly chosen. A random direction was then chosen for the emerging particle. The intersection points of the directions of the particle with the planes of

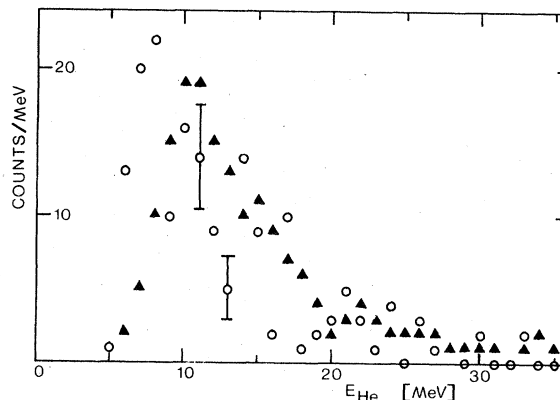


FIG. 2. Effect of correction for energy loss in target. The net energy spectrum from π^+ bombardment of Al, after background subtraction, is given by circles. Solid triangles represent the energy spectrum after the correction. Several statistical error bars are shown.

the detectors were then calculated. The ratio of the number of particles emitted within the surfaces of the detectors to the total number of emitted particles gave the effective solid angle. The overall uncertainty in the effective solid angle is about 10%.

The net spectra, obtained after background subtraction, had to be corrected for energy loss within the target volume. A Monte Carlo procedure was used for that purpose. For each particle hitting the telescope, a traversed target thickness was randomly chosen in the range set by target thickness, target inclination, and direction of motion of the particle as chosen above. Every particle in the spectrum was then assumed to have traversed that particular thickness. The initial energy of the particle (assumed to be an α particle) was calculated using the method of Zaidins,¹⁷ letting the particle have the measured energy when leaving the target. That calculation was repeated many times. The resulting spectrum was then normalized by division to the number of repetitions. The effects of this procedure are shown in Fig. 2, for a π^+ bombardment of Al: (a) The entire spectrum is shifted nonlinearly to higher energies; (b) the spectrum is smoothed out due to the statistical averaging procedure. The final energy resolution is 1–2 MeV. This procedure also introduced a distortion of the corrected energy spectra at low energies, near the instrumental cutoff. This effect is negligible for Ni, Ag, and Au, where the peak of the distribution is far from this cutoff. For C and Al, however, this distortion limits the reliability of the distribution to energies above about 10 MeV.

III. RESULTS AND ANALYSIS

The measured cross sections are summarized in Table I, and the energy distributions are shown in Figs. 3–6. The quoted uncertainties include both systematic and statistical errors. The cross section for π^- on aluminum agrees, within the experimental uncertainty, with that found in a preliminary measurement.¹¹

The descending part in the spectra from π^- bombardments is shown in Fig. 3. It is noticeable that all spectra exhibit the same features: a nearly exponential slope, roughly the same for all nuclei, and no specific structure. These characteristics are indicative of a statistical process of emission, in which specific features are washed out. Therefore, analysis of our data by comparison to evaporation calculations is suggested. The input for an evaporation simulation consists of an excited nucleus with a given excitation energy. We used an intranuclear cascade calculation to simulate the spectrum of nuclei and excitations.

We used the codes ISOBAR and EVA (IE),^{18,19} made available to us by Fraenkel, as modified somewhat by Zaider *et al.*¹ Detailed descriptions of the model and codes are given by the authors. This model has recently been used^{1, 2, 11, 12, 13} in the analysis of pion-induced inclusive reactions. We will now summarize briefly the features of the calculation.

The intranuclear cascade stage is a series of two-body interactions between pions, nucleons, and Δ isobars within the nucleus. The cascade is initiated by the interaction of the incident pion with a nucleon. Free nucleon data are used. Each product of the interactions is followed by the code until its energy falls below a cutoff energy, related to its separation energy. Pion absorption is assumed to take place through two interactions which involve nucleons and Δ isobars:



TABLE I. Measured cross sections for He ions.

Target	Projectile	He energy range (MeV)	$\left. \frac{d\sigma}{d\Omega} \right _{90^\circ}$ (mb/sr)
C	π^-	11.5–36.0	3.1 ± 0.7
	π^+	11.5–36.0	2.3 ± 0.5
Al	π^-	9.5–36.0	5.1 ± 1.2
	π^+	9.5–36.0	3.9 ± 0.9
Ni	π^-	7.5–36.0	13.1 ± 2.1
	π^+	7.5–36.0	8.3 ± 1.6
Ag	π^-	7.5–36.0	24.2 ± 4.0
Au	π^-	10.5–36.0	13.0 ± 3.0
	π^+	11.5–36.0	9.0 ± 3.0

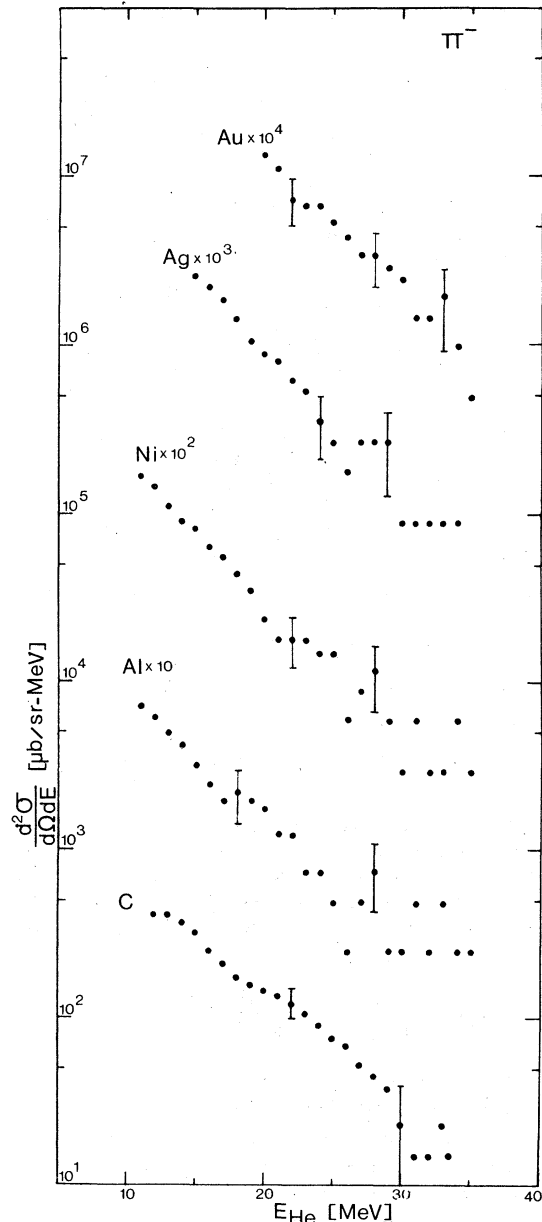


FIG. 3. Partial energy spectra of He ions from π^- bombardment. The low energy part of the spectra, up to the peak, is not shown. Several statistical error bars are shown.



Several single nucleons may be emitted during the cascade, leaving at the end of this stage a nucleus with a known excitation energy.

The excited nucleus is the input to the calculation of the evaporation stage. The emission probability per unit time of a particle j with a kinetic energy between ϵ to $\epsilon + d\epsilon$ is given in this stage by the following²⁰:

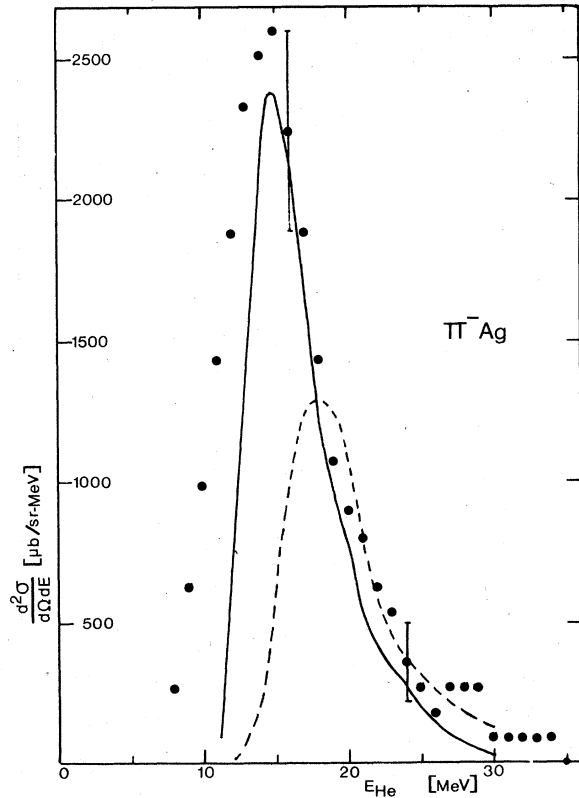


FIG. 4. Energy spectra of He ions from π^- bombardment of Ag. Several statistical error bars are shown. The lines are smooth approximations of the calculated He ions spectrum. Dashed line—first set of calculations; solid line—second set of calculations. See text.

$$P_j(\epsilon)d\epsilon = \frac{g_j m_j}{\pi^2 h^2} \sigma_{cj} \left| \frac{W(f)}{W(i)} \right| \epsilon d\epsilon, \quad (6)$$

where g_j and m_j are the number of spin states and mass of the emitted particle, respectively; σ_{cj} is the capture cross section for the formation of the emitting nucleus in the inverse reaction (i.e., the collision of the emitted particle with the residual nucleus); and $W(f)$ and $W(i)$ are the level densities of the residual and emitting nuclei, respectively. The capture cross section is found from the expression:

$$\sigma_{cj} = \sigma_G (1 + C_j) \left| 1 - \frac{k_j V_j}{\epsilon} \right|, \quad (7)$$

where σ_G is the geometric cross section and V_j is the height of the Coulomb barrier for particle j . C_j and k_j are parameters adjusted such as to yield the capture cross sections in the continuum theory.²¹ They are introduced to approximate roughly the effect of barrier penetration. The level density is calculated from the expression²⁰:

$$W(E) = C \exp[2(aE)]^{1/2}, \quad (8)$$

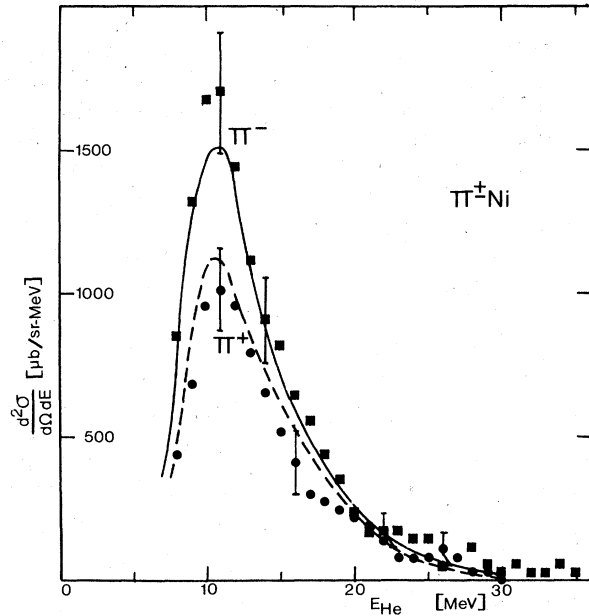


FIG. 5. Energy spectra of He ions from bombardments of Ni. Squares— π^- ; points— π^+ . Several statistical error bars are shown. The solid line (for π^-) and the dashed line (for π^+) are smooth approximations of the calculated He-ions spectra.

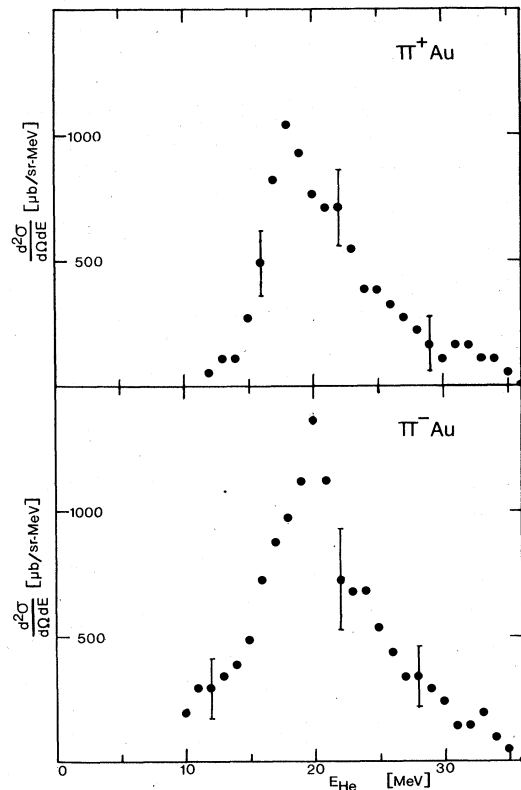


FIG. 6. Energy spectra of He ions from π^- and π^+ bombardments of gold. Several statistical error bars are shown.

where a is a level-density parameter.

The cascade and evaporation calculations assume the Fermi-gas model of the nucleus, which can hardly be used for light nuclei such as carbon. For heavy nuclei such as gold, on the other hand, the approximations in the evaporation calculation are not expected to be very reliable.²² Therefore, we do not present any results of calculations for either carbon or gold. The shape of the observed spectra from gold is similar to those of proton- and photon-induced α evaporation from gold.^{23, 24}

A first set of calculations was performed with standard parameters and code options as indicated by the authors^{18, 19} for best results. The gross shape of the spectra was reproduced by these calculations, but the parameters which describe evaporation spectra were not satisfactorily reproduced: (a) The calculated peak appeared at too high an energy; (b) the width of that peak did not reproduce the measured width; and (c) the cross sections at the peaks were lower than the measured ones. These disagreements are illustrated in Fig. 4, where we present the results of the first set of calculations for silver by a dashed line. A second set of calculations was then performed in order to get a better agreement with the experiment. The level-density parameter a was increased from $A/20$ MeV⁻¹ in the first set to $A/10$ MeV⁻¹. The effect of this change is threefold: to narrow the peak width, to lower the cross sections, and to increase slightly the peak energy. The parameter k_j was then decreased to increase the barrier-penetration probability, and to lower the peak energy to the experimental value. This change caused an increase of the calculated cross sections. The resulting spectrum for the silver target is shown by a solid line in Fig. 4. The improved agreement with experiment is noticeable. The results of the second set of calculations for the nickel target are shown by the lines in Fig. 5. They are in good agreement with the experimental spectra. For aluminum, the results of both sets of calculations reproduced the measured spectra reasonably well. The major differences between the two sets take place in the region of the expected peak. Unfortunately, the peak was not observed due to the experimental cutoff. In Table II we present a comparison of the measured cross sections to the calculated cross sections for the same energy range.

It is interesting to note that both π^- - and π^+ - induced spectra were reproduced by the calculations. It is thus shown that the differences between the π^- - and π^+ - induced spectra can be accounted for by the differences in the $\pi^\pm N$ interactions and by the Coulomb interaction in a classical treatment.

We note that a high value for a ($\approx A/10$ MeV⁻¹) is

TABLE II. Comparison of measured and calculated cross sections.

Target	Pion charge	Energy range (MeV)	Measured (mb/sr)	Calculated (mb/sr)
Al	π^-	9.5–30.0	4.9 ± 1.2	5.5
	π^+	9.5–30.0	3.7 ± 0.9	6.0
Ni	π^-	7.5–30.0	12.9 ± 2.0	12.0
	π^+	7.5–30.0	8.3 ± 1.6	9.0
Ag	π^-	7.5–30.0	23.8 ± 4.0	15.5

adequate for high excitation energies^{19, 25} (≈ 100 MeV); whereas a lower value for a ($\approx A/20$ MeV⁻¹)²⁵ suits lower excitation energies. Since the higher value seemed to give better results, this may be taken as a first indication of the important role of pion absorption in flight in reactions where He ions are emitted. We will return to this question in the next section.

It is not surprising that we got a better fit with a lower k_j . It is well known²⁶ from proton-induced reactions that in evaporation calculations the classical Coulomb barrier has to be reduced. Nuclear expansion and surface vibrations of the excited nucleus have been suggested as possible causes for the disagreement between experimental data and calculations, since these phenomena have the effect of lowering the barrier height.

IV. DISCUSSION

This paper deals with those processes in which α particles are emitted in the interaction of a pion with a nucleus. All our spectra and calculations refer to He ions rather than to α particles. However, in a preliminary experiment¹¹ we showed that ^3He contributes no more than 15% to the He spectra. The results of the IE calculation support this conclusion for all nuclei. Therefore, in our following discussion we will refer to α particles rather than to He ions.

A. α measurements

As previously mentioned, the IE calculations provide us with the possibility of singling out the contributions of well defined channels. They show that, for all considered nuclei and for both pion charges, about 90% of the α particles evaporate in processes where the pion was absorbed. This is consistent with our earlier remark in Sec. III that the use of the high excitation-energy approximation to the level-density parameter a indicates a major contribution from pion absorption in flight.

An event in which a pion is absorbed produces a highly excited nucleus. Considering the α spec-

tra, it is clear that the emission of an α particle hardly exhausts the available excitation energy. Therefore, it is likely that other particles are emitted as well, spreading the inclusive α cross section over several residual nuclei for which $\Delta A \approx 4$.

B. γ -ray measurements

Deexcitation γ -ray measurements yielded high relative cross sections for one- α -removal channels. This could suggest a large probability for real α emission. However, consider, for example, the interaction of π^- with aluminum [see reactions (1)–(3a) in Sec. I]. We select aluminum, since it is the only monoisotopic target used in both our α measurement and deexcitation γ -ray experiments. IE calculations predict here that real α particles are emitted in less than 10% of the reactions which lead to ^{23}Na . Therefore, on the basis of this cascade-evaporation model, it can be stated that one- α -removal lines, observed in deexcitation γ -ray experiments, do not necessarily imply large probability for real α emission.

C. Common channel

The one- α -removal reaction, reaction (1), has one channel, reaction (2a), which is common to both deexcitation γ -ray and to direct α methods of measurement. We mentioned in the beginning of this section that IE calculations predict that in α -emission processes all channels in which the pion was not absorbed contribute a total of about 10%. Since reaction (2a) corresponds to one such channel, its cross section is expected to be much smaller (less than 10%) than the total cross section for α emission. On the basis of Secs. A and B, we conclude that the common channel, reaction (2a), has a cross section which is much smaller than the total cross section for both the inclusive α measurement [reaction (1)] and the inclusive γ measurement [reaction (2)].

D. π^-/π^+ ratios

The cross-section ratios for bombardments with π^- and π^+ are listed in Table III. Within the experimental uncertainties, all ratios are greater than 1, indicating higher probability for α emission from π^- -induced reactions. The average ratio is about 1.4, equal to the ratio found for total cross sections in this pion-energy range.²⁷ This could be expected, since the α particles emerge in a wealth of exit channels, so that any specific features are washed out.

TABLE III. π^- to π^+ ratios of He cross sections:

$$\frac{d\sigma}{d\Omega}(\pi^-) / \frac{d\sigma}{d\Omega}(\pi^+).$$

Target	Experimental ^a	Calculated ^b
C	1.35 ± 0.32	
Al	1.31 ± 0.33	
Ni	1.58 ± 0.25	1.3
Au	1.44 ± 0.40	

^aIn same energy range for each ratio.

^bFrom differential cross sections. (See Table II).

V. CONCLUSIONS

The major conclusion which can be drawn from our results and analysis is that most of the low energy He particles from pion-induced reactions at 70 MeV are emitted in a process which can be successfully described by evaporation calculations. The results of the IE calculations emphasized the dominant role of pion absorption in flight in reactions in which α particles are emitted. The calculations have further shown that when a 70-MeV pion interacts, for example, with an ^{27}Al nucleus and a γ ($A=23$) is observed inclusively, there is small probability that an α particle is also emitted in the process. Conversely, if an α particle is observed inclusively, the reaction most likely does not yield a final product with $A=23$. On the basis of our model-dependent conclusions we wonder whether the results of previous inclusive deexcitation γ -ray experiments should be interpreted as suggesting a large probability for real α emission. A more definite statement can only be made as a result of systematic measurements of well defined exit channels.

VI. ACKNOWLEDGMENTS

It is our pleasure to thank those many people at the Centre d'Etudes Nucleaires de Saclay who joined their efforts to make this experiment possible: R. Letourneau with the electronics, B. Mahut with the targets, Mme. Garin with the detectors, and M. Godin and M. Adam with the vacuum system. We thank Dr. F. Netter and the team of the Accélérateur Linéaire de Saclay for the proper operation of the accelerator. Some of us would like to thank Dr. Ph. Catillon and the personnel of the Service de Physique Nucléaire à Haute Energie for the hospitality extended to them. We appreciate useful discussions with Dr. M. Moinester, Dr. C. Vinciguerra, and Dr. Z. Fraenkel. Two of us (A.D. and A.I.Y.) would like to thank the University of Illinois for the hospitality during the period in which the analysis was done.

- *Work supported in part by the Israeli Academy of Sciences and Humanities and by the U. S. National Science Foundation, Grant No. PHY 77-08100.
- †Permanent address: Argonne National Laboratory, Argonne, Illinois, 60439.
- ¹M. Zaider, D. Ashery, S. Cochavi, S. Gilad, M. A. Moinester, Y. Shamai, and A. I. Yavin, *Phys. Rev. C* **16**, 2313 (1977).
- ²B. J. Lieb, W. F. Lankford, S. H. Dam, H. S. Plendl, H. O. Funsten, W. J. Kossler, V. G. Lind, and A. J. Buffa, *Phys. Rev. C* **14**, 1515 (1976).
- ³D. Ashery, M. Zaider, Y. Shamai, S. Cochavi, M. A. Moinester, A. I. Yavin, and J. Alster, *Phys. Rev. Lett.* **32**, 943 (1974).
- ⁴H. E. Jackson, L. Meyer-Schützmeister, T. P. Wangler, R. P. Redwine, R. E. Segel, J. Tonn, and J. P. Schiffer, *Phys. Rev. Lett.* **31**, 1353 (1973).
- ⁵H. Ullrich, E. T. Boschitz, H. D. Engelhardt, and C. W. Lewis, *Phys. Rev. Lett.* **33**, 433 (1974).
- ⁶V. G. Lind, H. S. Plendl, H. O. Funsten, W. J. Kossler, B. L. Lieb, W. F. Lankford, and A. J. Buffa, *Phys. Rev. Lett.* **32**, 479 (1974).
- ⁷H. E. Jackson, D. G. Kovar, L. Meyer-Schützmeister, R. E. Segel, J. P. Schiffer, S. Vigdor, T. P. Wangler, R. L. Burman, D. M. Drake, P. A. M. Gram, R. P. Redwine, V. G. Lind, E. N. Hatch, O. H. Otteson, R. E. McAdams, B. C. Cook, and R. B. Clark, *Phys. Rev. Lett.* **35**, 641 (1975).
- ⁸P. J. Castleberry, L. Coulson, R. C. Minehart, and K. O. H. Ziock, *Phys. Lett.* **34B**, 57 (1971).
- ⁹C. W. Lewis, H. Ullrich, H. D. Engelhardt, and E. T. Boschitz, *Phys. Lett.* **47B**, 339 (1973).
- ¹⁰E. Bellotti, D. Cavalli, and C. Matteuzzi, *Nuovo Cimento* **18A**, 75 (1973).
- ¹¹A. Doron, J. Julien, M. A. Moinester, A. Palmeri, and A. I. Yavin, *Phys. Rev. Lett.* **34**, 485 (1975).
- ¹²J. F. Amman, P. D. Barnes, M. Doss, S. A. Dytman, R. A. Eisenstein, J. Penkrot, and A. C. Thompson, *Phys. Rev. Lett.* **35**, 1066 (1975).
- ¹³H. E. Jackson, S. B. Kaufman, L. Meyer-Schützmeister, J. P. Schiffer, S. L. Tabor, S. E. Vigdor, J. N. Worthington, L. L. Rutledge, Jr., R. E. Segel, R. L. Burman, P. A. M. Gram, R. P. Redwine, and M. A. Yates, *Phys. Rev. C* **16**, 730 (1977).
- ¹⁴Y. Y. Yam, *Phys. Rev. C* **11**, 73 (1975).
- ¹⁵V. M. Kolybasov, *Yad. Fiz.* **3**, 729 (1966) [*Sov. J. Nucl. Phys.* **3**, 535 (1966)]; V. M. Kolybasov, *Yad. Fiz.* **3**, 965 (1966) [*Sov. J. Nucl. Phys.* **3**, 704 (1966)]; V. M. Kolybasov and V. A. Tsepov, *Yad. Fiz.* **14**, 744 (1971) [*Sov. J. Nucl. Phys.* **14**, 418 (1972)].
- ¹⁶J. Hüfner, L. Tauscher, and C. Wilkin, *Nucl. Phys. A* **231**, 455 (1974).
- ¹⁷C. S. Zaidins, *Nucl. Instrum. Methods* **120**, 125 (1974).
- ¹⁸G. D. Harp, K. Chen, G. Friedlander, Z. Fraenkel, and J. M. Miller, *Phys. Rev. C* **8**, 581 (1973).
- ¹⁹I. Dostrovsky, Z. Fraenkel, and G. Friedlander, *Phys. Rev.* **116**, 683 (1959).
- ²⁰V. F. Weisskopf, *Phys. Rev.* **52**, 295 (1937).
- ²¹J. Blatt and V. F. Weisskopf, *Theoretical Nuclear Physics* (Wiley, New York, 1952); M. M. Shapiro, *Phys. Rev.* **90**, 171 (1953).
- ²²Z. Fraenkel (private communication).
- ²³G. Chenevert, I. Halpern, B. G. Harvey, and D. L. Hendrie, *Nucl. Phys. A* **122**, 481 (1968).
- ²⁴J.-O. Adler, G. Andersson, and H.-Å. Gustafsson, *Nucl. Phys. A* **223**, 145 (1974).
- ²⁵M. El Nadi and A. Hashem, *Phys. Rev. C* **13**, 2189 (1976).
- ²⁶L. Yaffe, *Nuclear Chemistry* (Academic, New York, 1968), Vol. 1, Chap. 3.
- ²⁷G. Burlison, K. Johnson, J. Calarco, M. Cooper, D. Haggerman, H. Meyer, R. Redwine, I. Halpern, L. Knutson, R. Marrs, M. Jakobson, and R. Jeppesen, in *Proceedings of the Sixth International Conference on High Energy Physics and Nuclear Structure*, Santa Fe and Los Alamos, June, 1975 (unpublished).